PLOS ONE

RESEARCH ARTICLE

Reactive/Less-cooperative individuals advance population's synchronization: Modeling of *Dictyostelium discoideum* concerted signaling during aggregation phase

Zahra Eidi[1]*, **Najme Khorasani**[1], **Mehdi Sadeghi**[2]

1 School of Biological Sciences, Institute for Research in Fundamental Sciences (IPM), Tehran, Iran,
2 National Institute of Genetic Engineering and Biotechnology (NIGEB), Tehran, Iran

* z.eidi@ipm.ir

OPEN ACCESS

Citation: Eidi Z, Khorasani N, Sadeghi M (2021) Reactive/Less-cooperative individuals advance population's synchronization: Modeling of *Dictyostelium discoideum* concerted signaling during aggregation phase. PLoS ONE 16(11): e0259742. https://doi.org/10.1371/journal.pone.0259742

Editor: Irene Sendiña-Nadal, Universidad Rey Juan Carlos, SPAIN

Received: May 16, 2021

Accepted: October 25, 2021

Published: November 18, 2021

Data Availability Statement: All relevant data are within the manuscript and its Supporting information files.

Funding: The author(s) received no specific funding for this work.

Competing interests: The authors have declared that no competing interests exist.

Abstract

Orchestrated chemical signaling of single cells sounds to be a linchpin of emerging organization and multicellular life form. The social amoeba *Dictyostelium discoideum* is a well-studied model organism to explore overall pictures of grouped behavior in developmental biology. The chemical waves secreted by aggregating *Dictyostelium* is a superb example of pattern formation. The waves are either circular or spiral in shape, according to the incremental population density of a self-aggregating community of individuals. Here, we revisit the spatiotemporal patterns that appear in an excitable medium due to synchronization of randomly firing individuals, but with a more parsimonious attitude. According to our model, a fraction of these individuals are less involved in amplifying external stimulants. Our simulations indicate that the cells enhance the system's asymmetry and as a result, nucleate early sustainable spiral territory zones, provided that their relative population does not exceed a tolerable threshold.

Introduction

Cell communication has marked a major transition in the evolution process of life complexity which resulted in multicellular organisms containing many cells acting in concert [1, 2]. This ability is coordinated by biochemical signaling networks within individual cells. This process becomes feasible via chemical signaling between fellow creatures. Once the same chemicals are being sensed and produced, every single cell in the population attunes itself to the presence and activities of other cells around it. This collective behavior can lead to the "emergence" of constructions, a new structure only created by a lot of individual interactions between single cells [3]. This is one of the most fascinating and mysterious features of evolutionary life. In particular, collective migration of cohesive cell groups is substantial in organizational constructions like embryogenesis, tissue formation, wound healing, and cancer invasion [4]. In addition, this collective behavior of unicellulars has been appealing to inspire the engineering of swarm robotics in recent years [5]. All the above complex emergent behaviors arise from a

relatively simple behavior of individual entities following a certain ruleset of interactions. The subsequent order and unification appear after the population density of signaling cells meets a threshold. It turns out that "more is different", but how many more cells are needed for synchronization to happen among the population and global signal propagation? Any answer to this question also might relate to the important ambivalence in the field of developmental biology that which one is precedent over the other: organization or differentiation? One of the well-established model organisms in developmental biology to address general views of communication, collective behavior, morphogenesis, and differentiation is the amoeba *Dictyostelium discoideum*. The amoeba is studied particularly as a borderline between one cell type and two. The cells are capable to evolve from a unicellular to a multicellular organism during their life-cycle by resorting to a chemical mechanism of intercellular communication [6]. During most of its life-cycle, the organism lives in the soil as a single amoeba and feeds on bacteria. When the nutrients are depleted, the cells secrete a chemical called cyclic adenosine monophosphate (cAMP) in response. This starts a multicellular developmental process [7]. Cells sense gradients of cAMP which has been emitted from their fellow creatures and direct their chemotactic movements towards regions of its higher concentration. They simultaneously amplify the environmental cAMP concentration by secreting it in their turn. The amplification dynamics results in a periodic cAMP wave propagation process in the medium. The waves propagate from the aggregation center outwardly and guide the chemotactic movement of other cells towards the locus. As a result, up to a million amoeboid cells stream towards the aggregation centers. Thereafter the system goes through a sequence of morphogenetic phases which ultimately land up a fruiting body consisting of two cell types: a delicate stalk of millimeter height, in which about 20% of the cells die to lift the mass of encapsulated spore cells up and hold them off the ground for optimal spore dispersal [8].

The biochemistry behind the process of signaling is acceptably well-understood [9]. The process starts after that the extracellular cAMP is bounded to the membrane's peripheral receptors. This triggers a chain of intracellular chemical reactions which leads to the production afresh of cAMP and its release into the extracellular medium. The cycle attains its terminus after degradation of cAMP by the enzyme phosphodiesterase, through which the receptors become free again [10]. In order to form the spatiotemporal patterns, it is necessary that the concentration of re-produced cAMP exceeds that of initially bounded to receptors. This happens through a non-linear autocatalytic process and thus comes at an expensive price [11]. However, during the aggregation process, each and every single cell of the population is confronted with the limits posed by the energetic costs of cellular metabolism for signaling and locomotion while it is in the starving phase of its life cycle [12]. Hence, naturally, they should be inclined to parsimoniously spend their energy, both at the individual and population levels. Although it is possible that the whole number of cells cooperate in signal relaying dynamics throughout the medium, it is a reasonable question to ask that if it is plausible for them to do so as energy-consuming units?

On the other hand, one of the crucial issues in the genesis of global coherent spatiotemporal patterns in a medium of randomly distributed signaling individuals is that how and why the system selects between circular and spiral waves to propagate chemical information from one point to another [13]. Circular waves generally appear as coherent activity of a group of individuals, which are referred as pacemakers. The cells spontaneously oscillate and send out periodic pulses of cAMP [14]. However, spiral waves emerge due to breaking the symmetry of interfacing circular patterns [15]. They are sustainable and not extinguished once they arise. Besides, the oscillation frequency of spiral waves is often higher than circular ones [14, 16]. In principle, the formation of spiral patterns provides a sustainable cue for the individuals to steer them toward a focal point [17].

Analysis of emerging cAMP waves during aggregation process of *Dictyostelium* shows that, while in areas with low population densities circular patterns are more favored, in zones with higher population densities spiral waves are preferred more [7, 13, 18, 19]; however, there are deviations from this observation [9, 20].

From a theoretical point of view, it has been shown that the presence of moderate levels of dynamical noise in a nonlinear system can result in enhanced signal strength [21], in the effect known as spatiotemporal stochastic resonance. In this study, we will discuss the effect of additive colored noise in construction of sustainable propagating waves in excitable medium. Here, we use excitable medium formalism as a general framework to elucidate general features of spatiotemporal patterns emerging from cell-cell signaling, plus an extra condition permitting the appearance of population bimodality. The basic idea of the model is an ansatz, which assumes that it is probably more affordable for the population if a fraction of cells contribute less in amplifying cAMP oscillations in the streaming aggregates and retain their energy for future population survival. We see that this assumption not only is profitable to spend the population's energy but also advances synchronization of individuals and as a result, earlier emerging sustainable spiral patterns, even in low population densities.

Materials and method

In general, an excitable medium is comprised of a continuous set of coupled locally excitable regions, i.e. cells, which can be both independently stimulated and inhibited. Each cell is characterized by the level of its local extracellular cAMP u and the state of its cAMP receptors v. The medium is capable of transmitting information (u value) via promoting spatiotemporal cAMP wave patterns within itself [22]. Components of this medium enjoy of having two distinguishable states: rest and excited. An individual's rest state can be raised to the excited state, provided that the concentration of diffusive stimulus secreted by its neighbors exceeds a threshold. The cell plays the same excitatory role for its adjacent cells in turn and this process initiates a propagating excitation wave throughout the medium. The main dynamical features of a broad class of excitable media can be simulated by a two-component reaction-diffusion system of the form [23]

$$\frac{\partial u}{\partial t} = f(u, v) + \nabla^2 u, \tag{1}$$

$$\frac{\partial v}{\partial t} = u - v + \eta(t). \tag{2}$$

in which the local kinetics of the activator u and the inhibitor v is governed by the nonlinear functions $f(u, v)$ in Eq 1 and the linear function $u - v$ in Eq 2, respectively. We assume that $f(u, v) = \epsilon^{-1}u(1 - u)(u - u_{th})$, where $u_{th} = (v + b)/a$. The parameter ϵ indicates excitability of the system which is the time-scale difference between the fast excitatory variable u and the slow refractory variable v while a and b are the controlling parameters of the model. Our numerical simulations are based on a slightly modified version of Barkley model [24]. In our model, we assume that a given cell is in its excited state if its corresponding value of u exceeds the size of boundary layer δ, See Fig 1A.

In Eq 2, the function $\eta(t)$ reflects affected noise on the inhibitor variable v. We assume that η is driven by a colored noise known as Ornstein–Uhlenbeck process with $\frac{\partial \eta}{\partial t} = -\lambda\,\eta + \sqrt{2\,D\lambda}\,\zeta(t)$, which has intensity D and correlation time λ^{-1}. Here, $\zeta(t)$ is Gaussian white noise of mean zero and correlation function $<\zeta(t)\zeta(s)> = \delta(t - s)$ [25].

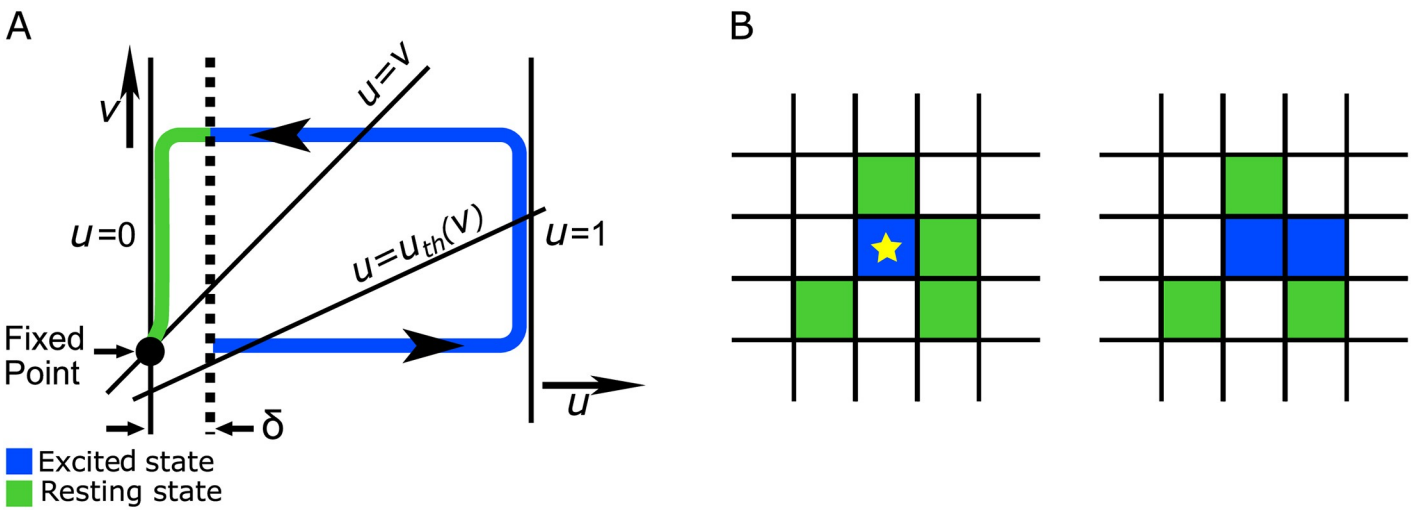

Fig 1. (Color online) schematic illustration of local dynamics. Corresponding dynamics of the excitable system in uv-plane is depicted by its nullclines. The u nullcline includes three separate lines: $u = 0$, $u = 1$ and $u = (v + b)/a$, while the line $u = v$ is the v nullcline. The dotted line indicates the boundary layer δ which all the initial conditions within it decay to the fixed point. The itinerary in the uv- plane starts haphazardly once the value of u exceeds the amount of δ. Eventually, the itinerary returns to the fixed point after passing a large excursion, adapted from [24] (A). The medium consists of excitable cells spatially connected to each other by a diffusion-like coupling. An exited cell (the blue asterisk unite) is capable of triggering excitation through its neighbors with the help of diffusing cAMP molecules (B).

https://doi.org/10.1371/journal.pone.0259742.g001

The local dynamics of an excitable medium, that is the dynamics in the absence of diffusion, See Fig 1A, is characterized by a stable but excitable fixed point. The point sits at the intersection locus of u and v nullclines, which are the answers of $f(u, v) = 0$, and $u - v = 0$ line respectively. Fig 1A provides a schematic illustration of typical corresponding nullclines. Small perturbations of the rest state decay and return to the fixed point immediately. However, perturbations that exceed the boundary layer size δ increase and decay only after the system has performed a large excursion in the uv-phase plane. In this case, after passing a long loop the system relaxes to the fixed point and stands by for the next itinerary.

A special feature of a spatially extended system of excitable media is that such systems promote local impulses i.e. leading to propagating spatiotemporal patterns throughout the system. In reality, this takes place provided that the diffusive coupling of the excitable elements is of adequate strength. The diffusive mechanism with which adjacent excitatory cells stimulate each other via signaling messenger u is schematically illustrated in Fig 1B. Here the blue asterisked unit is in its excited state while all its nearby cells relax in their rest state, .i.e. they are green. The strength of the diffusion of the local u is sufficient to impel one of at rest neighbors cell, say its right neighbor, into its excited state, as depicted in Fig 1B. The excited state of the blue cell soon becomes refractory, a state in which the cell neither stimulates nor is stimulated by its neighbors. Note that the cells have to be close enough so that diffusion of signaling messenger works constructively to share the information of the amount of u from one cell to the other.

As a matter of fact, the nonlinear cubic term $f(u, v)$ in Eq 1 is necessary to shape patterns. An evident feature in the aggregation of *Dictyostelium* amoebae is that the environmental cAMP signals are amplified by the individuals [6]. But, what if there are a fraction of the individuals which are less involved in amplifying external stimulants? Let us suppose that the population of aggregating cells is not pure, but mixed including two types based on their tendency to treat proactive/cooperative or reactive/less-cooperative behavior in the population. A group of cells are capable (and tend) to boost the external cAMP signaling messenger via secreting more cAMP locally; This way, they form pacemakers that trigger periodic pulses of cAMP in

the medium. This is modeled by the nonlinear term in the Eq 1. We refer to this group of individuals as proactive/cooperative cells. The other type of cells is potentially unable to amplify the environmental cAMP concentration. Thus, they are reactive/less-cooperative. These individuals align their locomotion toward the gradient of the chemical stimulus, utilizing the signal released by other cells. Based on the model, the same set of equations as Eq 1 governs the dynamics of reactive/less-cooperative cells except that instead of the cubic term in this equation, they possess a linear term as $u - u_{th}$. Now, the question is that, considering the energy cost of nonlinear behavior and time limitations during which intercellular biochemical reactions occur to form spatiotemporal patterns, what is the ideal combination of the cells in the mixed population? In other words, assuming that the population density of the whole population is ϕ_1 and among these cells, a fraction of ϕ_2 are reactive/less-cooperative ones, what is the optimum value of ϕ_2 by which the system can bear the subsistence of the cells before depriving spatiotemporal patterns totally?

Results

Population density of individuals has to meet a threshold for global spatiotemporal patterns appearance

Circular and spiral waves are two generic spatiotemporal patterns of excitable systems. Depending on the system's initial condition and interacting parameters, the spatial diversity distribution of individuals and frequencies of oscillatory elements the corresponding features of circular waves or spiral ones are favored by the medium [19]. The aim of current investigation is to study the probable presence of a mixed population at the early stages of cell aggregation. Accordingly, we restrict the simulations only to the wave propagation properties upon which even in high densities of a single species population the shape of patterns are circular. For a thorough list of parameters see section S1 Appendix. Shown in Fig 2 are spatiotemporal snapshots of different lattices exclusively composed of proactive/cooperative cells with different population densities ϕ_1. From Fig 2, this is apparent that for low pure population densities ($\phi_1 < 0.4$), the local chemoattractant cAMP concentration is insufficient to synchronize the individuals in a way that global territory zones of patterns form. Throughout this study, we focus our attention on the system whose at least $\phi_1 = 0.4$ fraction of its lattice units are covered with cells.

Spiral waves appear in a field composed of the mixed population even at low population densities

One of the most striking features of non-pure bimodal populations is the emergence of spiral waves at low population densities. Fig 3 panels: 3A, 3D, 3G, 3J, 3M shows time-lapse frames of

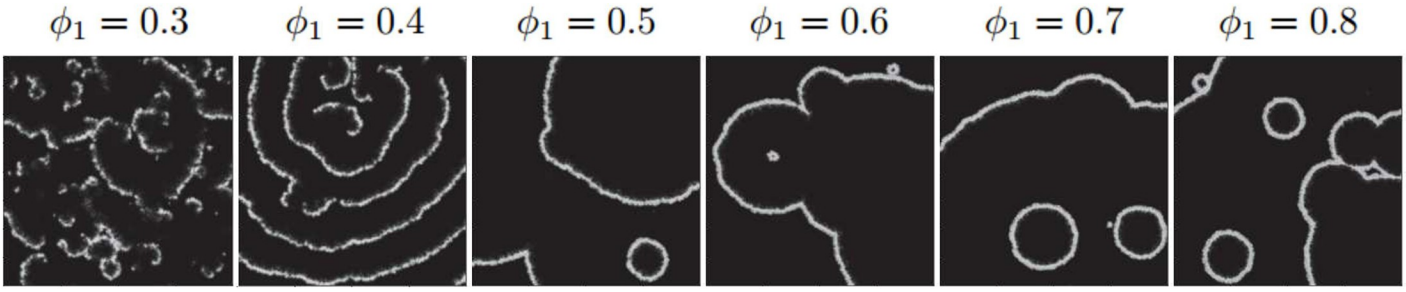

Fig 2. Emergent patterns on different lattices including randomly distributed firing cells with variant ϕ_1. ϕ_1 is population density of the cells which determines the number density of occupied units on the lattices of size 400 × 400. Here, the cells are exclusively of proactive/cooperative type. All parameters of the model are kept the same for these systems and listed in section S1 Appendix.

https://doi.org/10.1371/journal.pone.0259742.g002

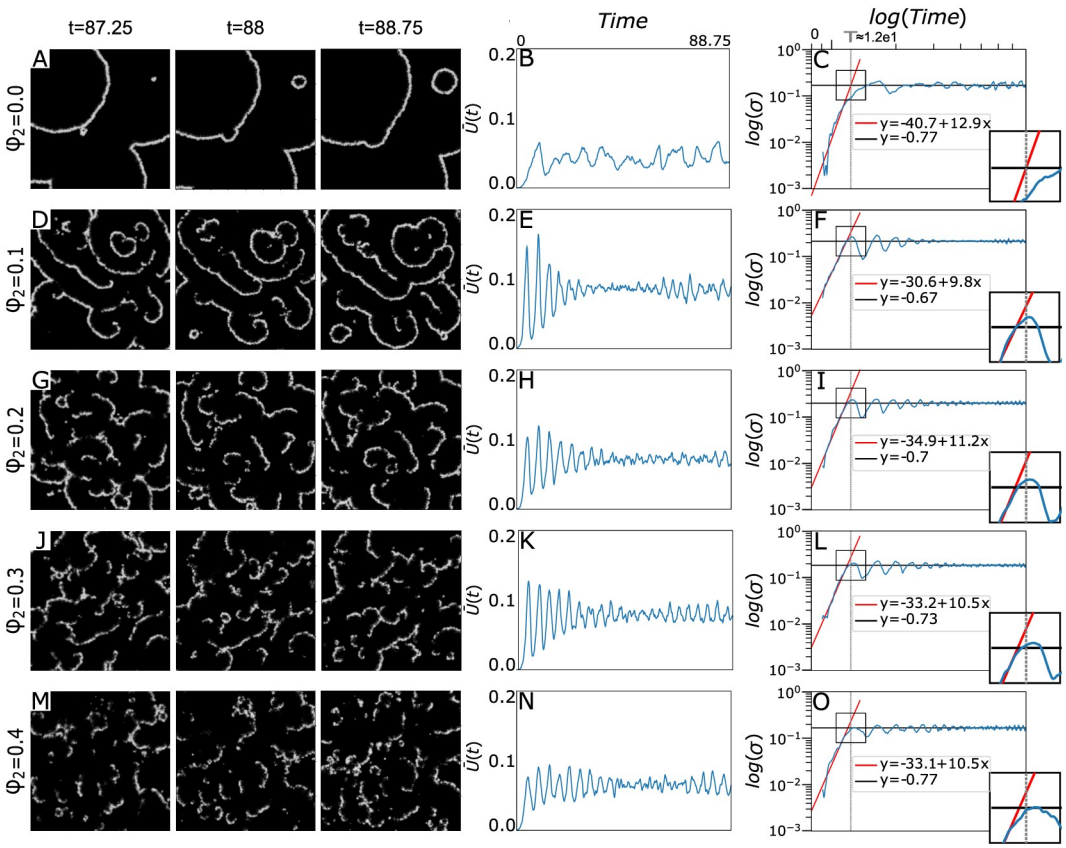

Fig 3. (Color online) Propagating wave through a system with $\phi_1 = 0.5$ and $\phi_2 = 0.0$ (A), $\phi_1 = 0.5$ and $\phi_2 = 0.1$ (D), $\phi_1 = 0.5$ and $\phi_2 = 0.2$ (G), $\phi_1 = 0.5$ and $\phi_2 = 0.3$ (J) and $\phi_1 = 0.5$ and $\phi_2 = 0.4$ (M). There are 60 iteration interval between the illustrated subsequent patterns, here 'it' is an abbreviation for iteration. Emerging spiral waves are distinguishable only at (D) See also S1 to S6 Videos. Mean concentration of signaling agent, calculated as $\bar{u}(t) = \frac{1}{N^2}\sum_{ij} u_{ij}(t)$ where $u_{ij}(t)$ is the cAMP concentration of point (i, j) at time t, in a system with $\phi_1 = 0.5$ and $\phi_2 = 0.0$ (B), $\phi_1 = 0.5$ and $\phi_2 = 0.1$ (E), $\phi_1 = 0.5$ and $\phi_2 = 0.2$ (H), $\phi_1 = 0.5$ and $\phi_2 = 0.3$ (K) and $\phi_1 = 0.5$ and $\phi_2 = 0.4$ (N). Logarithmic scale of standard deviation of u, calculated as $\sigma(t) = \left[\frac{1}{N^2}\sum_{ij}(u_{ij}(t) - \bar{u}(t))^2\right]^{1/2}$, for a system with $\phi_1 = 0.5$ and $\phi_2 = 0.0$ (C), $\phi_1 = 0.5$ and $\phi_2 = 0.1$ (F), $\phi_1 = 0.5$ and $\phi_2 = 0.2$ (I), $\phi_1 = 0.5$ and $\phi_2 = 0.3$ (L) and $\phi_1 = 0.5$ and $\phi_2 = 0.4$ (O). Red and black lines are representatives of growing phase and oscilatory one, respectively. In each plot red line is the linear regression of $\log(\sigma(t))$ for the first 300 iterations of every simulation. Black line in each diagram is the mean value of $\log(\sigma(t))$ in the last 3000 iterations in each simulation. The magnified window located in right bottom of panels C, F, I, L and O illustrates the crossover time of the system dynamics between these two regimes. The vertical gray dashed line corresponds to the crossover time in a pure system with $\phi_1 = 0.5$ and $\phi_2 = 0.0$ which is the intersection point of black and red lines in panel (C).

https://doi.org/10.1371/journal.pone.0259742.g003

spatiotemporal patterns appearing in systems with different ϕ_2 values, where just half of the lattice units are occupied,. i.e. population density of all systems are $\phi_1 = 0.5$. Fig 3A illustrates appearing and disappearing circular waves where the whole cells are proactive ones ($\phi_2 = 0$) and panels D, G, J, and M show signaling patterns of systems in which population density of reactive/less-cooperative individuals are none-zero with the ϕ_2 value indicated beside each row, See also S1 to S5 Videos. The difference of these patterns becomes exquisite when a small fraction of cells (say $\phi_2 = 0.1$) are of reactive/less-cooperative type, Fig 3D, where spiral patterns emerge, S2 Video. Indeed, it seems in bimodal populations with a low population density of reactive cells, circular waves interact with one another setting up into spiral waves. However, when the reactive population density exceeds the threshold value of $\phi_2 = 0.1$, the waves extinguish just to fluctuate in local cAMP concentration and the distinguishable spiral waves disappear gradually.

To assess the concentration level of signaling messenger u, we compute the mean-field concentration of the stimulant in the medium as $\bar{u}(t) = \frac{1}{N^2}\sum_{ij} u_{ij}(t)$ where $u_{ij}(t)$ is the cAMP concentration of point (i, j) at time t. It seems that even in the presence of the reactive/less-cooperative cells the average concentration of stimulants remains intact, between 0.05 and 0.08, Compare trend value of $\bar{u}(t)$ plot in panels: B, E, H, K, and N of Fig 3. This brings us to the conclusion that the situation of the system has not change for the worse in this case after making the population bimodal. The concentration standard deviation, which is the root mean squared fluctuation in the cAMP chemical concentration reads as $\sigma(t) = \left[\frac{1}{N^2}\sum_{ij}(u_{ij}(t) - \bar{u}(t))^2\right]^{1/2}$. Comparison of panels C, L, I, F, and O of Fig 3 persuade us that the behavior of time evolution of stimulant concentration standard deviation is almost identical in each case. It has typically two regions separated by a crossover time, which is the intersection point of two lines defining two distinct dynamical behavior. The concentration width initiates by growing exponentially and after passing the crossover time, its dynamics follows an oscillating behavior around some saturated value. The saturated regime occurs during the very time period that the spatiotemporal waves are observable in the medium. In Fig 3, the crossover time of the system which only includes proactive/cooperative cells, T, is illustrated as a dashed line. The line is considered as a benchmark against which one can decide about the same quantity in other systems and inspect the impact of the presence of reactive/less-cooperative cells on the quantity. Remarkably, the crossover time between two growing and oscillating regimes occurs earlier when reactive/less-cooperative cells attend in the medium. One may conclude that reactive/less-cooperative individuals advance the population's synchronization to construct spatiotemporal patterns.

The growth slope of the plots before crossover time is indicated inside each panel, see panels C, L, I, F, and O of Fig 3. The quantity is a measure of how fast the fluctuating dynamics of concentration evolve to reach out the oscillatory dynamics. It seems that the slope has descending behavior with respect to the presence of reactive individuals. At the beginning of each simulation, only firing cells which are randomly distributed throughout the network are in excited state and all other cells are at rest state. Thus, averaging out the value of u on the whole network gives random fluctuating values in successive times. After a while, signaling messengers diffuse to neighbor cells and make them excited. When a sufficient number of cells become excited, the spatiotemporal oscillating patterns emerge. Indeed, as a result of diffusion of u the amplitude of cAMP fluctuations descends. However, since every individual swings between the two excited and rest states, the mean value of u in the network permanently fluctuates, even if with smaller amplitude.

Mere presence of reactive/less-cooperative individuals do not affect population's synchronicity markedly

As an important illustration of the general features of collective signalling, we consider the cross-correlation S for the u variable as space and time-averaged nearest-neighbor distance of all elements, normalized by the total spatial amplitude variance [26]. The quantity measures the coherency of the patterns and is defined as $S = \langle\frac{Cov(t)}{\sigma^2(t)}\rangle_t$ where $Cov(t)$ is spatial auto-covariance of nearest neighbors at time t elucidated as $Cov(t) = N^{-2}\sum_{ij}\frac{1}{4}\sum_{b\in N_{ij}}(u_{ij} - \bar{u})(b - \bar{u})$. Here, b takes up u values of all 4 elements of a von Neumann neighborhood N_{ij} at each lattice site and the bracket $\langle\rangle_t$ denotes averaging over the total integration time t. This is a quantitative measure for the relative change of the order in a spatially extended system. Its maximal value is $S = 1$ for a completely synchronized network in space and time. Table 1 provides details about the S value for variant pairs of reactive and proactive mixture in a medium in which half of its surface is covered with the cells. The three rows of the table represent the S value of three

Table 1. Comparison of *S* values of the media with different proportions of reactive/less-cooperative cells whose surface is covered with randomly distributed firing cells with population density $\phi_1 = 0.5$.

	$\phi_2 = 0$	$\phi_2 = 0.1$	$\phi_2 = 0.2$	$\phi_2 = 0.3$	$\phi_2 = 0.4$	$\phi_2 = 0.5$
S	0.949	0.940	0.940	0.940	0.938	0.936
	0.949	0.939	0.939	0.939	0.938	0.936
	0.950	0.940	0.940	0.938	0.938	0.936

https://doi.org/10.1371/journal.pone.0259742.t001

independent realizations for each simulated system. Comparing the first array of each row, which belongs to a system in the absence of reactive individuals, with other ones in each array, we see that the *S* value experiences a modest decline (around 0.01) in presence of reactive cells. However, this quantity hardly changes and remains fairly constant when the fraction of reactive cells increases in the medium. The survey of the value for a bunch of systems with variant pairs of ϕ_1 and ϕ_2 reveals that the *S* value for the whole systems are between 0.930 and 0.950.

Low proportions of reactive/less-cooperative individuals in a population contribute to the formation of sustainable spiral waves

Fig 4 illustrates arranged snapshots of a dozen mixed populations with different pairs of ϕ_1 and ϕ_2, which are addressed on vertical and horizontal margins, respectively. The disposition of snaps in the array suggests that not only arising circular or spiral patterns are not erratic, but also it can provide a methodical ordering to predict the related pattern of every pair of population mixture. As depicted in Fig 4 in pure populations (with $\phi_1 \geq 0.4$) with parameters listed in S1 Appendix circular waves are favored. This category is marked with a blue boundary in the figure. It seems that the concentration of signaling messenger cAMP in the pure system with $\phi_1 = 0.3$ is not high enough to form distinguishable patterns. Although the pattern of the pure system with $\phi_1 = 0.4$ sounds to be circular, due to apparent differences with other pure systems, See Supplemental S1 to S7 Videos, we excluded it from the blue border. From left to right we have an ascending amount of reactive/less-cooperative cells in the populations and simultaneously, a descending order in the patterns. In the territory of the red border in which a low fraction of cells is of reactive/less-cooperative type spiral waves appear. It seems that low amounts of these cells in the medium enhances the system asymmetry and promote the early nucleation of spiral forms. However, the system can tolerate subsistence of these cells only up to a threshold depending on the population density of whole cells, e.g., the threshold is around $\phi_2 = 0.2$ in the system with $\phi_1 = 0.8$. When the relative number of these cells increases in the population the patterns become more inconspicuous gradually until only a fine mist of dilute signals come into sight at the right side of the array, see the area restricted with yellow and orange boundary lines in Fig 4).

Discussion

The oscillatory signals during the self-aggregation period of *Dictyostelium discoideum* are reinforced through two major processes: intracellular biochemical feedback loops that make the cells relay the external signals, and cell recruitments in response to the signals which, in turn, leads to configurations with more efficacy in signaling [3]. Here, we merely concentrate on the first process and adjourn the second one to the next studies. In the current study, we implemented a parsimonious attitude to model a concerted signaling process through a mixed population of randomly distributed excitable coupled individuals. Based on the model, the population is composed of two types of cells: Proactive/cooperative cells which contribute toward relaying external signaling messenger of cAMP, and reactive/less-cooperative ones that

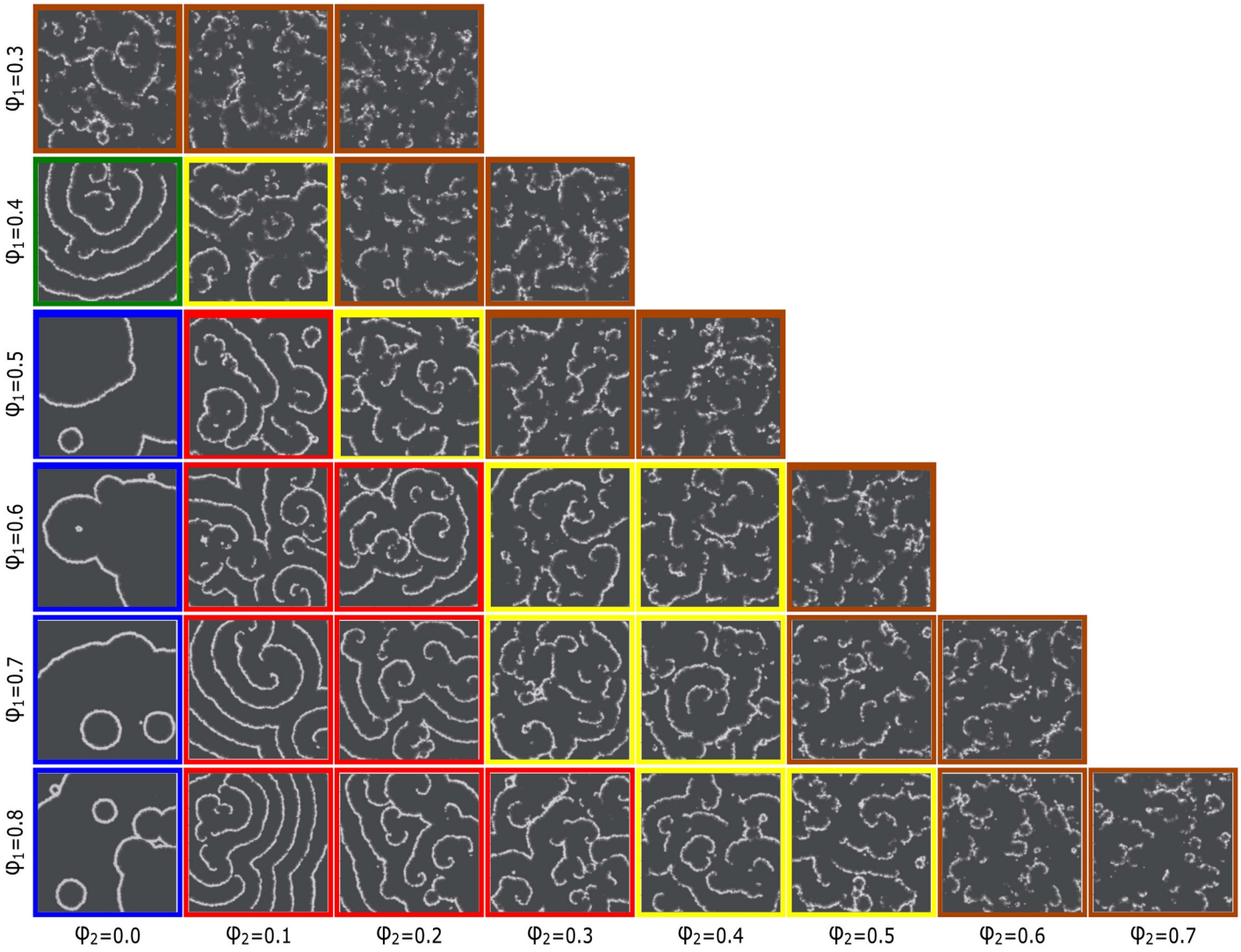

Fig 4. (Color online) disposition of pattern snapshots on a common instance of time in lattices of 400 × 400 size, covered with mixed populations with different pairs of ϕ_1 and ϕ_2. ϕ_1 is the population density of the whole cells on each lattice and ϕ_2 is the fraction of reactive/less-cooperative cells among the population. The related row and column of each pattern in the array are appointed by their ϕ_1 and ϕ_2 indicated in vertical and horizontal margins, respectively. For example, the bottom row includes the systems with the same population density of individuals $\phi_1 = 0.8$ but with a variant fraction of reactive/less-cooperative ones ϕ_2. Similar patterns are enclosed with a colored border. Pure systems are arranged in the first column.

https://doi.org/10.1371/journal.pone.0259742.g004

less contribute to relay the environmental cAMP. Population bimodality can emerge even when biological processes are homogenous at the cell level and the environment is kept constant [27]. There are pieces of evidence that cheating occurs in mixed populations of wild clones [3, 28]. Although selfish behavior known as cheating is reported in the slug stage, one might track back its trace to prior stages of social communication and interaction between individual units that are spatially separated, as well [6].

One of the fundamental difficulties in simulating fast-slow dynamics in excitable media is the separation of corresponding time scales of excitatory and recovery variables in such systems. In the model that we have implemented here, for the cooperating individuals, within the excited region the time scale of u can be very fast due to the small parameter ϵ. Accordingly, in simulating such systems, care must be taken to prevent numerical instabilities and to preserve

the qualitative character of the fast jumps in u. However, within the recovery region the dynamics are very simple. The excitation variable u is essentially zero, so that the local dynamics effectively reduces to exponential decay of the recovery variable v. Moreover, in the interior of these regions, diffusion is negligible because the spatial profile of u is basically flat. It is worth to mention that the size of boundary layer, δ, within which u vanishes equals to 10^{-4}. The algorithm has been chosen both for simplicity and for efficient numerical implementation [24]. Our model has an extra feature which is presence of non-cooperative cells whose dynamics read as follows:

$$\begin{aligned}\frac{\partial u}{\partial t} &= u - u_{th} + \nabla^2 u \\ \frac{\partial v}{\partial t} &= u - v + \eta(t) \\ \frac{\partial \eta}{\partial t} &= -\lambda\,\eta + \sqrt{2\,D\lambda}\,\zeta(t).\end{aligned}$$

where $u_{th} = (v + b)/a$. Here, the lack of ϵ in the equations makes the governed dynamics slower than that of cooperative cells. On the other hand, the η term which adds up to v is a mean-reverting process of Ornstein–Uhlenbeck type and inhibits u from growing exponentially. Fig 5 illustrates the square root of u along amid row pixels of our network during the last 2000 iterations of simulations for different combination of cooperator and non-cooperator cells. It is seen that the value of u for none of the pixels exceeds from the maximum which is demonstrated by red color.

Since secretion of every single cAMP molecule involves the coordination of a cascade of metabolic processes including expression and synthesis of regulatory enzymes [29], overproduction of the signaling messenger could increase the metabolic cost of signal production. The sociomicrobial idea behind constructing our model is that, as the secreted signals that are produced by a group of individuals have benefits that are available to all of the cells in a population, the strategy with which the same spatiotemporal patterns are accessible with lower secretion of signaling molecule is more favorable [30].

Experiments show that in non-living reaction-diffusion systems such as the Belouzov–Zhabotinsky reaction, oscillators often form around inhomogeneities [31]. In contrast, evolving systems covered by populations of *Dictyostelium* are intrinsically heterogeneous. Their variant kinetic properties during the course of time have a profound impact on waveform competition [15]. Noise and variability in the form of cell-to-cell differences are common themes in the study of biological organizations. Essentially, instead of suppressing or filtering out the noise and eliminating diversity, individual living matters often exploit these features to drive many of theirs intracellular and extracellular processes [3, 32]. Differences between pattern formation in biological and chemical or physical systems are attributed to these properties [32]. Principally, self-organized physical systems consist of functionally identical elemental parts, while components in that of biological systems are diverse in their essence [33]. From the biochemistry of secretion of signals [9], we know that the relaxation time is short but not negligible. White noise has no time-correlations, and is thus appropriate to model systems with negligible relaxation time. Thus, it seems that a colored noise like the Ornstein–Uhlenbeck process is a more realistic model of the actual input to the state of its cAMP receptors v [25]. This process is Markovian. This might not be obvious since although we deal with a first-order equation $\frac{\partial \eta}{\partial t} = -\lambda\,\eta + \sqrt{2\,D\lambda}\,\zeta(t)$, we have an extra time-dependent noise $\zeta(t)$. The noise is however, uncorrelated and thus does not introduce a statistical dependence on the past. The Ornstein–Uhlenbeck process exhibits an exponentially decaying correlation function, is also known in

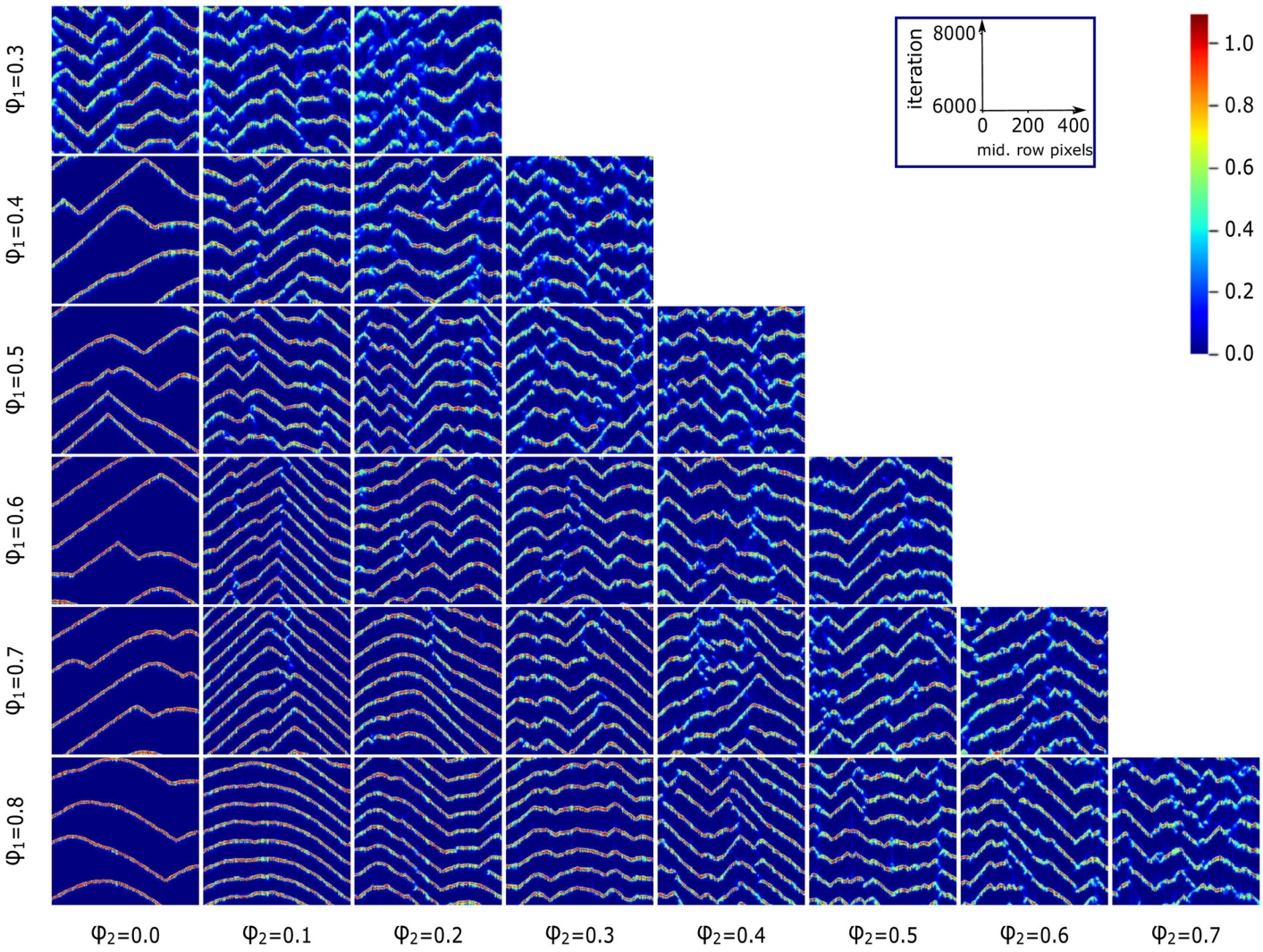

Fig 5. The square root of u concentration along amid row pixels of the networks during the last 2000 iterations of simulations in lattices of 400 × 400 size, covered with mixed populations with different pairs of ϕ_1 and ϕ_2. ϕ_1 is the population density of the whole cells on each lattice and ϕ_2 is the fraction of reactive/less-cooperative cells among the population. The related row and column of each pattern in the array are appointed by their ϕ_1 and ϕ_2 indicated in vertical and horizontal margins, respectively.

https://doi.org/10.1371/journal.pone.0259742.g005

the mathematical literature as a "mean-reverting" process and when adds up to v variable, keeps its growth balanced. Besides, λ has units of frequency and gives a measure of the cutoff frequency of the fluctuations of the noise, which is by definition of the order of ϵ value.

Recently, it has been shown that stable activity centers appear spontaneously in areas of higher cell density with the oscillation frequency of these centers depending on their density [18]. On the other hand, it has been proved that diversity-induced resonance has a principal role in pattern competition between circular and spiral waves [34]. In particular, the increase and decrease of the spiral wave count with increasing diversity are statistically regulated by the number of oscillatory elements in the lattice, rather than by the frequency differences between target and spiral waves [19]. In our model, the individuals essentially enjoy of an inherent inhomogeneity due to the bimodal nature of the population, i.e. composed of reactive/less-cooperative cells and proactive/cooperative ones. As it is evident in Fig 2 circular wave frequencies in different systems covered only by proactive/cooperative individuals are identical.

Accordingly, after substituting a fraction of these cells with reactive ones, one can attribute the emerging patterns of spirals to the intrinsic inhomogeneity of cells, especially at low population densities, see Fig 3. This consequence is likely to be of help to explain why for a particular strain and circumstance one pattern tends to dominate. This is an important question because they bear on early events governing the self-aggregation of the slime mold organizational process. Any answer to this question might shed indirect light on the classic question that: Which one comes first? Differentiation or Morphogenesis.

From experimental insight, it is traditionally viable to measure the amount of local concentration of cAMP relay by light scattering waves caused by the synchronized cell movements at variant developmental stages of *Dictyostelium* aggregation [35–37]. However, there are reports that show no clear evidence exists for cAMP relay organizing collective cell migration at multicellular stages [38]. Most recent experiments report cAMP waves in living cell populations using cAMP specific fluorescence resonance energy transfer (FRET) techniques during aggregation process [7, 39]. On the other hand, Hashimura, et.al challenged the traditional view about the role of cAMP relay in the organization of collective cell migration recently [40].

It is seen that Table 1 cannot reflect quantitatively the apparent differences between the forming patterns in the presence and absence of reactive cells, Fig 4, although it is a well-defined and recurring quantity to measure synchronicity degree of a network [26]. This may suggest that a generalized version of this quantity is needed for quantifying the synchronicity of a mixed population networks in practice. To the best of our knowledge, there is not such a generalization in the related literature.

In our in silico experiments, apparent resemblances of emerging patterns in different systems are deemed to classify them, see Fig 4. To abandon ourselves from the likely occurring errors of manual monitoring, it is necessary to develop an automated machine learning-based method of data analysis and image processing to compare the patterns and set them out in Fig 4. Nevertheless, it sounds that $\frac{\phi_2}{\phi_1}$ reckoned to be a relevant quantity in apparent similarities between the snapshots of different systems. Another relevant quantity in shared features of patterns in the presence and absence of reactive/less-cooperative cells is the growth incline of cAMP concentration standard deviation, panel *C* in comparison with panels *F*,*I*, *L*, and *O*. The apparent diminution of the slope of red lines in the presence of reactive individuals reminds us of different methods of deposition of colloidal aggregates resulting in vastly different exponential growth slopes of the width of mean height, where the slopes define universality classes of roughening processes [41]. Certain statement about this requires a thorough survey and would be a potentially interesting area for future research.

Supporting information

S1 Appendix. Numerical simulation and data analysis.
(PDF)

S1 Video. Simulation of a system with whole population density $\phi_1 = 0.5$ and reactive cells density $\phi_2 = 0.0$. The whole related parameters of this simulation have been implemented based on the ones which are listed in the S1 Appendix.
(MP4)

S2 Video. Simulation of a system with whole population density $\phi_1 = 0.5$ and reactive cells density $\phi_2 = 0.1$. The whole related parameters of this simulation have been implemented based on the ones which are listed in the S1 Appendix.
(MP4)

S3 Video. Simulation of a system with whole population density $\phi_1 = 0.5$ and reactive cells density $\phi_2 = 0.2$. The whole related parameters of this simulation have been implemented based on the ones which are listed in the S1 Appendix.
(MP4)

S4 Video. Simulation of a system with whole population density $\phi_1 = 0.5$ and reactive cells density $\phi_2 = 0.3$. The whole related parameters of this simulation have been implemented based on the ones which are listed in the S1 Appendix.
(MP4)

S5 Video. Simulation of a system with whole population density $\phi_1 = 0.5$ and reactive cells density $\phi_2 = 0.4$. The whole related parameters of this simulation have been implemented based on the ones which are listed in the S1 Appendix.
(MP4)

S6 Video. Simulation of a system with whole population density $\phi_1 = 0.5$ and reactive cells density $\phi_2 = 0.5$. The whole related parameters of this simulation have been implemented based on the ones which are listed in the S1 Appendix.
(MP4)

S7 Video. Simulation of a system with whole population density $\phi_1 = 0.4$ and reactive cells density $\phi_2 = 0.0$. The whole related parameters of this simulation have been implemented based on the ones which are listed in the S1 Appendix.
(MP4)

Author Contributions

Conceptualization: Zahra Eidi, Mehdi Sadeghi.

Data curation: Zahra Eidi, Najme Khorasani.

Formal analysis: Zahra Eidi, Najme Khorasani, Mehdi Sadeghi.

Investigation: Zahra Eidi, Najme Khorasani, Mehdi Sadeghi.

Methodology: Zahra Eidi, Mehdi Sadeghi.

Project administration: Zahra Eidi, Najme Khorasani, Mehdi Sadeghi.

Resources: Zahra Eidi.

Software: Najme Khorasani.

Supervision: Zahra Eidi, Mehdi Sadeghi.

Validation: Zahra Eidi, Najme Khorasani.

Visualization: Najme Khorasani.

Writing – original draft: Zahra Eidi.

Writing – review & editing: Zahra Eidi, Najme Khorasani, Mehdi Sadeghi.

References

1. Herron MD, Michod RE. Evolution of complexity in the volvocine algae: Transitions in individuality through Darwin's eye. Evolution. 2008; 62:436–451. https://doi.org/10.1111/j.1558-5646.2007.00304.x PMID: 18031303
2. Queller DC. Relatedness and the fraternal major transitions. Philos Trans R Soc Lond B Biol Sci. 2000; 355:1647–1655. https://doi.org/10.1098/rstb.2000.0727 PMID: 11127911

3. Reid CR, Latty T. Collective behaviour and swarm intelligence in slime moulds. FEMS Microbiology Reviews. 2016 Nov; 40(6):798–806. https://doi.org/10.1093/femsre/fuw033 PMID: 28204482
4. Friedl P, Gilmour D. Collective cell migration in morphogenesis, regeneration and cancer. Nat. Rev. Mol. Cell Biol. 2009; 10:445–457. https://doi.org/10.1038/nrm2720 PMID: 19546857
5. Parhizkar M, Serugendo GM. Agent-based models for first- and second-order emergent collective behaviors of social amoeba *Dictyostelium discoideum* aggregation and migration phases. Artificial Life and Robotics Journal. 2018; 23(4): 498–507. https://doi.org/10.1007/s10015-018-0477-3
6. Kessin RH. Dictyostelium: evolution, cell biology, and the development of multicellularity. Cambridge University Press; 2001.
7. Singer G, Araki T, and Weijer CJ. Oscillatory cAMP cell-cell signalling persists during multicellular *Dictyostelium* development. Commun. Biol. 2019; 2:139. https://doi.org/10.1038/s42003-019-0371-0 PMID: 31044164
8. Brock DA, Gomer RH. A cell-counting factor regulating structure size in *Dictyostelium*. Genes Dev. 1999; 13(15):1960–1969. https://doi.org/10.1101/gad.13.15.1960 PMID: 10444594
9. Pálsson E, Cox EC. Origin and evolution of circular waves and spirals in *Dictyostelium discoideum* territories. Proc. Natl Acad. Sci. USA. 1996 Feb 6; 93(3):1151–5. https://doi.org/10.1073/pnas.93.3.1151 PMID: 8577731
10. Iglesias PA. Feedback control in intracellular signaling pathways: Regulating chemotaxis in *Dictyostelium discoideum*. European Journal of Control. 2003; 9(2-3):227–36.
11. Scott S. K., Chemical Chaos. Oxford University Press, Oxford; 1991.
12. Strassmann JE, Queller DC. Evolution of cooperation and control of cheating in a social microbe. Proc. Natll. Acad. Sci. 2011; 108(2):10855–10862. https://doi.org/10.1073/pnas.1102451108
13. Lee KJ, Goldstein RE, Cox EC. cAMP waves in *Dictyostelium* territories. Nonlinearity. 2002; 15: C1–C5. https://doi.org/10.1088/0951-7715/15/1/601
14. Gregor T, Fujimoto K, Masaki N, Sawai S. The onset of collective behavior in social amoebae. Science. 2010 May; 328(5981):1021–5. Epub 2010 Apr 22. https://doi.org/10.1126/science.1183415 PMID: 20413456
15. Lauzeral J, Halloy J, Goldbeter A. Desynchronization of cells on the developmental path triggers the formation of spiral waves of cAMP during *Dictyostelium* aggregation Proc. Natl Acad. Sci. 1997; 94 (17):9153–9158. https://doi.org/10.1073/pnas.94.17.9153
16. Sgro AE, Schwab DJ, Noorbakhsh J, Mestler T, Mehta P, Gregor T. From intracellular signaling to population oscillations: bridging size- and time-scales in collective behavior. Mol Syst Biol. 2015; 11:779. https://doi.org/10.15252/msb.20145352 PMID: 25617347
17. Noorbakhsh J, Schwab DJ, Sgro AE, Gregor T, Mehta P. Modeling oscillations and spiral waves in *Dictyostelium* populations. PHYSICAL REVIEW E. 2015 Jun; 91(6):062711. https://doi.org/10.1103/PhysRevE.91.062711 PMID: 26172740
18. Vidal-Henriquez E, Gholami A. Spontaneous center formation in *Dictyostelium discoideum*. Scientific Reports. 2019; 9:3935. https://doi.org/10.1038/s41598-019-40373-4 PMID: 30850709
19. Grace M, Hütt MT. Pattern competition as a driver of diversity-induced resonance. Eur. Phys. J. B. 2014; 87,29. https://doi.org/10.1140/epjb/e2013-40873-8
20. Durston AJ. *Dictyostelium discoideum* aggregation fields as excitable media. J. Theor. Biol. 1973; 42: 483–504. PMID: 4358315
21. McDonnell MD and Abbott D, What Is Stochastic Resonance? Definitions, Misconceptions, Debates, and Its Relevance to Biology. PLoS Comput. 2 Biol. 2009. 5,e1000348. https://doi.org/10.1371/journal.pcbi.1000348 PMID: 19562010
22. Sager BM. Propagation of traveling waves in excitable media. Genes Dev. 1996; 10:2237–2250. https://doi.org/10.1101/gad.10.18.2237 PMID: 8824584
23. Murray JD. Mathematical Biology II, Springer; 2003.
24. Barkley D. A model for fast computer simulation of waves in excitable media. Physica D. 1991; 49:61–70. https://doi.org/10.1016/0167-2789(91)90194-E
25. Laing C, Lord CJ. Stochastic Methods in Neuroscience, Oxford University Press, New York; 2010.
26. Busch H, Kaiser F. Influence of spatiotemporally correlated noise on structure formation in excitable media. Phys. Rev. E. 2003; 67, 041105. https://doi.org/10.1103/PhysRevE.67.041105 PMID: 12786345
27. Fernandez-de-Cossio-Diaz J, Mulet R,Vazquez A. Cell population heterogeneity driven by stochastic partition and growth optimality. Scientific Reports. 2019; 9,9406. https://doi.org/10.1038/s41598-019-45882-w PMID: 31253860

28. Strassmann JE, Zhu Y, Queller DC. Altruism and social cheating in the social amoeba *Dictyostelium discoideum*. Nature. 2000; 408,965–7. https://doi.org/10.1038/35050087 PMID: 11140681

29. Kriebel PW and Parent CA. Adenylyl Cyclase Expression and Regulation During the Differentiation of *Dictyostelium Discoideum*. IUBMB Life. 2004, 56(9): 541–546. https://doi.org/10.1080/15216540400013887 PMID: 15590560

30. Asfahl KL and Schuster M. Social interactions in bacterial cell–cell signaling. FEMS Microbiology Reviews. 2017, fuw038, 41,92–107 https://doi.org/10.1093/femsre/fuw038 PMID: 27677972

31. Agladze K, Keener JP, Müller Sc, Panfilov A. Rotating spiral waves created by geometry. Science. 1994; 264,1746. https://doi.org/10.1126/science.264.5166.1746 PMID: 17839908

32. Grace M, Hütt MT. Regulation of Spatiotemporal Patterns by Biological Variability: General Principles and Applications to *Dictyostelium discoideum*. PLOS Computational Biology. 2015; 11(11):e1004367. https://doi.org/10.1371/journal.pcbi.1004367 PMID: 26562406

33. Grace M, Hütt MT. Predictability of spatio-temporal patterns in a lattice of coupled FitzHugh–Nagumo oscillators. J R Soc Interface. 2013 Jan 24; 10(81):20121016. https://doi.org/10.1098/rsif.2012.1016 PMID: 23349439

34. Glatt E, Gassel M, Kaiser F. Variability-sustained pattern formation in subexcitable media. PHYSICAL REVIEW E. 2007; 75: 026206. https://doi.org/10.1103/PhysRevE.75.026206 PMID: 17358404

35. Alcantara F, Monk M. Signal propagation during aggregation in the slime mould *Dictyostelium discoideum*. J. Gen. Microbiol. 1974; 85:321–334. https://doi.org/10.1099/00221287-85-2-321 PMID: 4615133

36. Rietdorf J, Siegert F, Weijer CJ. Analysis of optical density wave propagation and cell movement during mound formation in *Dictyostelium discoideum*. Dev. Biol. 1996; 177:427–438. https://doi.org/10.1006/dbio.1996.0175 PMID: 8806821

37. Dormann D, Weijer CJ. Propagating chemoattractant waves coordinate periodic cell movement in *Dictyostelium* slugs. Development. 2001; 128:4535–4543. https://doi.org/10.1242/dev.128.22.4535 PMID: 11714678

38. Wang B, Kuspa A. *Dictyostelium* development in the absence of cAMP. Science. 1997; 277:251–254. https://doi.org/10.1126/science.277.5323.251 PMID: 9211856

39. Kamino K, Kondo K, Nakajima A, Monda-Kitahara M, Kaneko K, Sawai S. Fold-change detection and scale invariance of cell-cell signaling in social amoeba. Proc. Natl. Acad. Sci. USA. 2017; 114:E4149–E4157. https://doi.org/10.1073/pnas.1702181114 PMID: 28495969

40. Hashimura H, Morimoto YV, Yasui M, Ueda M. Collective cell migration of *Dictyostelium* without cAMP oscillations at multicellular stages. Commun. Biol. 2019; 2,34. https://doi.org/10.1038/s42003-018-0273-6 PMID: 30701199

41. Barabasi AL, Stanley HE. Fractal Concepts in Surface Growth. Cambridge University Press; 1995.